Mechanism for Anomalous Hall Ferromagnetism in Twisted Bilayer Graphene

Nick Bultinck, Shubhayu Chatterjee, and Michael P. Zaletel

Phys. Rev. Lett. **124**, 166601 — Published 21 April 2020

DOI: 10.1103/PhysRevLett.124.166601

A mechanism for anomalous Hall ferromagnetism in twisted bilayer graphene

Nick Bultinck,[1,*] Shubhayu Chatterjee,[1,*] and Michael P. Zaletel[1,2]

[1] *Department of Physics, University of California, Berkeley, CA 94720, USA*
[2] *Materials Sciences Division, Lawrence Berkeley National Laboratory, Berkeley, California 94720*

Motivated by the recent observation of an anomalous Hall effect in twisted bilayer graphene, we use a lowest Landau level model to understand the origin of the underlying symmetry-broken correlated state. This effective model is rooted in the occurrence of Chern bands which arise due to the coupling between the graphene device and its encapsulating substrate. Our model exhibits a phase transition from a spin-valley polarized insulator to a partial or fully valley unpolarized metal as the bandwidth is increased relative to the interaction strength, consistent with experimental observations. In sharp contrast to standard quantum Hall ferromagnetism, the Chern number structure of the flat bands precludes an instability to an inter-valley coherent phase, but allows for an excitonic vortex lattice at large interaction anisotropy.

Moiré graphene systems are a class of simple van der Waals heterostructures [1] hosting interaction driven low-energy physics, making them an exciting platform to advance our understanding of correlated quantum matter. In twisted bilayer graphene (TBG) with a small twist angle between adjacent layers, interaction effects are enhanced by van Hove singularities coming from 8 nearly flat bands around charge neutrality (CN) in the Moiré- or mini-Brillouin zone (mBZ) [2–21]. Observation of correlated insulating states when 2 or 6 of the 8 TBG flat bands are filled confirms the importance of interactions [22–28].

Recent experiments indicate that certain magic angle graphene devices have large resistance peaks at $\nu = 0, 3$, with the latter featuring an anomalous Hall (AH) effect detected via hysteresis in the Hall conductance as a function of the out-of-plane magnetic field [29]. The Hall conductance is of order e^2/h but not yet quantized. Some have detected an meV-scale gap at CN, and a hysteretic behaviour of the Hall conductance with applied field at $\nu = -1$ [30]. In this work we discuss how the breaking of the 180-degree rotational symmetry (C_{2z}) by a partially aligned hexagonal boron-nitride (h-BN) substrate could explain these observations. A variety of works [31–37] have found that h-BN opens up a band gap at the Dirac points of graphene whose magnitude depends on the graphene / h-BN alignment angle, reaching $\Delta_{AB} \sim 17$meV [37] to ~ 30meV [35, 36] at perfect alignment. Notably, even in seemingly unaligned devices with little or no observable h-BN induced Moiré potential, band gaps of several meV are still observed [36, 37]. In TBG, the substrate can likewise gap out the band Dirac points at the $K_\pm$ points of the mBZ, splitting the bands as $8 = 4+4$ to create a gap at CN. We find that for certain sublattice splittings the resulting flat bands have Chern number $C = \pm 1$. This makes the TBG case similar to ABC stacked trilayer graphene, where under an appropriately directed electric field the flat bands have Chern numbers ± 3 [38].

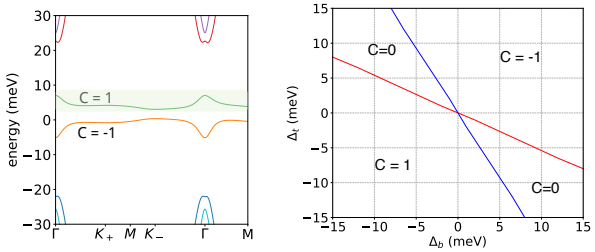

(a) (b)

FIG. 1: The effect of sublattice splittings Δ_t and Δ_b on the spinless single-valley Moiré Hamiltonian (SVMH). (**a**) Band structure around CN for $\Delta_t = 15$ meV and $\Delta_b = 0$. The flat band above (below) CN has Chern number $C = -1$ ($C = 1$). (**b**) Phase diagram of the SVMH for different Δ_t and Δ_b. Phases are labeled by the Chern number C of the flat $\tau = +$ conduction band. Blue (red) transition lines are characterized by a Dirac cone at the K_- (K_+) point of the mBZ.

Accounting for the C_{2z}-breaking substrate, the basic structure of the problem is as follows. The gap at CN allows us to focus only on the four nearly degenerate conduction (valence) bands for fillings above (below) CN, i.e, $\nu > 0$ ($\nu < 0$). These four Chern bands are uniquely labeled by their valley $\tau = +, -$ and spin $s = \uparrow, \downarrow$; time-reversal switches the valley index and enforces opposite Chern numbers for bands from opposite valleys. Since a $|C| = 1$ band is topologically equivalent to a Landau level (LL), the problem is roughly analogous to a spinful bilayer quantum Hall problem with one flux quanta per unit cell, but with opposite layers (valleys) experiencing opposite magnetic fields. The LLs are degenerate, but as in a quantum Hall ferromagnet (QHFM)[39] at integer filling the electrons may open a gap by spontaneously polarizing into a subset of these LLs, or a coherent superposition of them. In conventional quantum Hall bilayers at filling $\nu = 1$, interactions generically drive inter-layer coherence, e.g., the exciton condensate [40, 41]. But the twist here is the opposing Chern numbers of the two valleys. We find that the Chern number structure provides a topological reason for penalizing a coherent state: an exciton condensate between $C = 1, -1$ bands is analogous

[*] N.B. and S.C. contributed equally to this work.

to a superconductor in a strong magnetic field, which forces vortices into the order parameter, reducing the gain in the correlation energy. Hence, a spontaneously valley-polarized (VP) state is stable and exhibits AH effect with Hall resistance $\sim h/e^2$ (QAH if completely spin and valley polarized). Further, pinning of valley-polarization by an out-of-plane B^z due to a large orbital g-factor explains the presence of the R_{xy} hysteresis loop observed in Ref. [29].

The possibility of spin and valley polarization and/or quantum anomalous Hall physics and chiral edge states in TBG has been discussed previously in Refs. [38, 42–50], albeit from a different perspective. We also note that a recent self-consistent Hartree-Fock (HF) treatment of the continuum model exhibits *spontaneous* $C_{2z}T$ breaking at CN, though the resulting Chern numbers were $C = \pm 2$ [46].

Substrate-induced Dirac mass and Chern numbers– We model the effect of the h-BN substrate [31] by including in our band calculations a uniform but C_{2z} breaking A-B sublattice splitting Δ_t and Δ_b on the top and bottom layer respectively (see [51] for details). While h-BN may also introduce a Moiré potential, its magnitude falls off much more rapidly with alignment angle than $\Delta_{t/b}$ [37]. For our calculations we used a twist angle $\theta \approx 1.05^\circ$, and have taken a phenomenological corrugation effect into account by using a larger AB/BA inter-layer hopping w_1 as compared to the AA/BB inter-layer hopping w_0. Taking $w_0/w_1 = 0.85$ results in flat bands separated from the dispersing bands by an energy gap of approximately 20 meV (for zero sublattice splittings).

With sublattice splitting, the phases of the $\tau = +$ valley (or K-valley of monolayer graphene) Moiré Hamiltonian for different parameter regimes of Δ_t and Δ_b are shown in Fig. 1. We find four different regions where both Dirac cones in the mBZ are gapped because of the sublattice splittings. In these regions, there are two isolated flat bands. We find that these four regions have bands with Chern numbers [52] $C = \pm 1$ or $C = 0$, and are separated from each other by a Dirac point at either the K_- or K_+ point in the mBZ. In Fig. 1 we show the Chern number of the flat band for the $\tau = +$ valley above (below) CN in green (orange). The Chern number for the flat bands from the $\tau = -$ valley can be obtained by time-reversal.

The location of the $C = \pm 1$ phases can be understood from the fact that for small $\Delta_t = \Delta_b > 0$ or $\Delta_t = \Delta_b < 0$, the leading order effect of the sublattice potentials is to generate Dirac masses with the same sign at both the K_- and K_+ points of the mBZ. Because both Dirac cones in a single valley have the same chirality, this leads to bands with Chern number ± 1, a feature earlier work dubbed a "flipped Haldane model"[53] (see also [54–56]). From Fig. 1 we see that even if only one of the layers has a non-zero sublattice splitting, the strong inter-layer coupling ensures that both Dirac cones at the mBZ K-points acquire a mass.These findings can also be inferred analytically within the "chiral" approximation of tBLG [57, 58], in which all bands are sub-lattice polarized and carry Chern number $C = \sigma\tau$, where σ denotes sublattice.

Metal - valley polarization competition– In this work, we focus only on the four flat *conduction* bands above the CNP (the highlighted band in Fig. 1 and its valley and spin counterparts). In the supplement, we numerically justify this for TBG, showing that $\Delta_t \sim 15$ meV ($\Delta_b = 0$) creates a 30 meV gap between valence and conduction bands [51]. To phenomenologically model the effect of interactions in this set of bands we adopt a lowest Landau level (LLL) description. We can map the Chern bands to a LLL by constructing the Wannier-Qi states [51, 59, 60]. In the following, we use an approximation where the Wannier-Qi states of the flat bands are replaced by the continuum LLL wave functions of a two-dimensional electron gas. Physically, this amounts to neglecting the inhomogeneous Berry curvature in the Chern bands. The AH effect and edge transport reported in Ref. 29 can be explained if there is one VP hole per Moiré unit cell. From the data in Ref. [29] is not possible to exclude a spin-unpolarized, gapless phase. If the spins do polarize however, the underlying mechanism is expected to be the same as in conventional QHFM [39], and is not sensitive to the opposite Chern numbers of the two valleys. Therefore, in the analysis below we ignore spin and focus on the mechanism of valley polarization. Considering the uniform repulsive nature of the projected Coulomb interaction and the numerical evidence against stripes in the LLL [61], we disregard the possibility of interaction-induced charge density waves, and focus on the competition between valley-polarized, inter-valley coherent and metallic phases. For this we need to introduce two parameters in our LLL toy model: the bandwidth and the interaction anisotropy. To achieve a non-zero bandwidth we use a square lattice potential, that sidesteps the complexities of a hexagonal lattice and allows analytical progress.

We consider a torus of length L_x (L_y) in the x (y) direction, with a magnetic field perpendicular to the surface. We choose units in which $L_x L_y = 2\pi N_\phi l_B^2 \equiv N_\phi a^2$, where N_ϕ is the number of flux quanta piercing the torus, and $l_B = (\hbar/eB)^{-1/2}$ is the magnetic length. In particular, we will take $L_x = N_x a$ and $L_y = N_y a$, with $N_\phi = N_x N_y$. Next to the magnetic field, we also add a periodic potential $V_P(x, y) = w(\cos(2\pi x/a) + \cos(2\pi y/a))$, such that there is exactly 2π flux in each unit cell. The potential is invariant under translations over a in both the x and y-direction, which means that the momenta $k_x = n\frac{2\pi}{N_x a}$ and $k_y = n\frac{2\pi}{N_y a}$ ($n \in \mathbb{Z}$) are good quantum numbers.

We are interested in the physics in the LLL with Chern numbers $C = 1, -1$. The electron creation operator projected in these subspaces takes the form $\psi_\pm^\dagger(x, y) = \frac{1}{\sqrt{L_y l_B \sqrt{\pi}}} \sum_k e^{iky - \frac{1}{2l_B^2}(x \mp k l_B^2)^2} c_{\pm,k}^\dagger$, where we have chosen the Landau gauge which explicitly preserves (continuous) translation symmetry in the y-direction, such that $k = 2\pi n/L_y = 2\pi n/N_y a$ with $n \in \{0, 1, \ldots, N_x N_y\}$. We

now proceed in analogy to Ref. 62, and define the Bloch states $c^\dagger_{\pm,(k_x,k_y)} = c^\dagger_{\pm,\mathbf{k}}$ as

$$c^\dagger_{\pm,\mathbf{k}} = \frac{1}{\sqrt{N_x}} \sum_{n=0}^{N_x-1} e^{\pm i k_x (k_y+nQ) l_B^2} c^\dagger_{\pm,k_y+nQ}\,, \qquad (1)$$

where $Q = \sqrt{2\pi}/l_B = 2\pi/a$. The density operator in the LLL $n_\pm(\mathbf{q}) = \int \mathrm{d}\mathbf{r}\, e^{-i\mathbf{q}\cdot\mathbf{r}} \psi^\dagger_\pm(\mathbf{r})\psi_\pm(\mathbf{r})$ takes the form

$$n_\pm(\mathbf{q}) = F(\mathbf{q}) \sum_{k_x,k_y} e^{\pm i q_y k_x l_B^2} c^\dagger_{\pm,\mathbf{k}-\mathbf{q}/2} c_{\pm,\mathbf{k}+\mathbf{q}/2}\,, \quad (2)$$

where the form factor is given by $F(\mathbf{q}) = e^{-\mathbf{q}^2 l_B^2/4}$. In the Bloch basis, the Hamiltonian term associated with the periodic potential takes the diagonal form $H^p = \sum_{\mathbf{k}} \varepsilon_{\mathbf{k}} (c^\dagger_{+,\mathbf{k}} c_{+,\mathbf{k}} + c^\dagger_{-,\mathbf{k}} c_{-,\mathbf{k}})$, with $\varepsilon_{\mathbf{k}} = -we^{-\pi/2}[\cos(k_x a) + \cos(k_y a)]$.

We are interested in the effect of density-density interactions on the LLL electrons moving in the periodic potential, described by the following Hamiltonian:

$$H^i = \frac{1}{2N_\phi} \sum_{\mathbf{q},\tau,\tau'} V_{\tau,\tau'}(\mathbf{q}) : n_\tau(\mathbf{q}) n_{\tau'}(-\mathbf{q}), \qquad (3)$$

where we neglect the small inter-valley scattering terms [51]. We will consider a general repulsive interaction of the form $V(\mathbf{q})F^2(\mathbf{q}) = u_0(\mathbf{q})(\mathbb{1} + \tau^x) + u_1(\mathbf{q})(\mathbb{1} - \tau^x)$. In analogy to quantum Hall ferromagnetism [39, 40, 63] and related strongly coupled systems [64, 65], at half-filling of the two bands we expect that the main effect of H^i is to introduce a valley Hund's coupling between the electrons resulting in an insulating ground state. On the other hand, the *kinetic* term H^p coming from the periodic potential favors a metal over the VP insulator. To study the competition between these two phases, we perform a HF analysis using Slater determinants with correlation matrix $\langle c^\dagger_{\tau,\mathbf{k}} c_{\tau',\mathbf{k}'}\rangle = \delta_{\tau,\tau'}\delta_{\mathbf{k},\mathbf{k}'}\Theta(\epsilon^\tau_F - \epsilon_{\mathbf{k}})$, such that $\sum_\tau \sum_{\mathbf{k}} \Theta(\epsilon^\tau_F - \epsilon_{\mathbf{k}}) = N_\phi$. The possibility of inter-valley coherent states is addressed in the next section. For each Slater determinant, we define the corresponding valley polarization P_v as $P_v = (N_+ - N_-)/N_\phi$, where N_+ (N_-) is the number of electrons in the + (−) valley. Without loss of generality, we restrict to $P_v > 0$.

We first consider an isotropic ($u_1(\mathbf{q}) = 0$) dual-gate screened Coulomb potential with LLL form factors $u_0(\mathbf{q}) = 2\pi U e^{-\mathbf{q}^2 l_B^2/2} \tanh(d|\mathbf{q}|)/|\mathbf{q}|$, and screening length $d = a$. Using this interaction potential, we calculated the HF energy E^{HF} [51]. We find that for $W/U \lesssim 0.6$, where $W \equiv 4we^{-\pi/2}$ is the bandwidth, the completely VP state indeed has the lowest energy. When $W/U \approx 0.6$, the valley polarization P_v of the optimal Slater determinant jumps and starts decreasing continuously, indicating a first-order Mott transition from the VP insulator to an itinerant valley-ferromagnet. Around $W/U \approx 2.0$, P_v continuously goes to zero and a conventional metallic phase sets in [51].

Inter-valley coherence and exciton vortex lattice– In bilayer QH ferromagnets, the insulating layer-polarized state is unstable to a uniform exciton condensate or inter-layer coherent state in presence of infinitesimal interaction anisotropy $u_1(\mathbf{q}) > 0$ [40]. The situation here is different as even with $u_1(\mathbf{q}) = 0$, there is no SU(2) valley symmetry because of the Chern number mismatch. The VP state therefore only breaks discrete symmetries, indicating there will be no instability of this insulating state. Another, more physical, way to understand the absence of an exciton condensation instability is to use an analogy with type II superconductors. Because electrons in bands with an opposite Chern numbers effectively see opposite magnetic fields, an electron-hole condensate $\Delta(\mathbf{r}) = \langle c^\dagger_{+,\mathbf{r}} c_{-,\mathbf{r}}\rangle$ will behave like a charge 2e superconducting order parameter in a perpendicular magnetic field. However, in our scenario a Meissner-like effect, corresponding to uniform amplitude of the exciton order parameter, is ruled out from the outset. Rather, the magnetic field must leak through vortices in the exciton order parameter, leading to an excitonic vortex lattice phase. In this section, we show that both the VP insulator and the unpolarized metal are energetically favorable to the exciton vortex lattice, for sufficiently small interaction anisotropy $u_1(\mathbf{q})$.

For our LLL model, we can derive an exact expression for the exciton vortex lattice order parameter $\Delta(\mathbf{r})$. To respect all symmetries of the square lattice, we expect $\Delta(\mathbf{r})$ to have vortices at both the lattice sites and the plaquette centers, leading to a 4π vorticity in each unit cell. In the analytically tractable limit, we can uniquely determine $\Delta(\mathbf{r})$ up to a translation by demanding its invariance under the magnetic translations $\mathcal{T}(a\hat{x})$ and $\mathcal{T}\left(\frac{a}{2}(\hat{x}+\hat{y})\right)$, connecting the anticipated vortices [51]. In Fig. 2 we plot the magnitude of $\Delta(\mathbf{r})$ thus obtained, from which we clearly see the expected Abrikosov vortex lattice. Projecting $\Delta(\mathbf{r})$ to the LLL Bloch basis wavefunctions $\phi_{\pm,\mathbf{k}}(\mathbf{r})$ leads to a diagonal order parameter

$$\Delta_{\mathbf{k}} = \Delta_0 \sum_{j=-\infty}^{\infty} e^{-i\frac{\pi}{2}j^2} e^{-\frac{1}{4}(2k_y+jQ)^2 l_B^2 - ik_x(2k_y+jQ)l_B^2} \quad (4)$$

where Δ_0 represents the overall strength of the exciton condensate. $\Delta_{\mathbf{k}}$ has two nodes with identical phase winding at $\mathbf{k} = \pm(\pi/2, -\pi/2)$, as shown in Fig. 2 [51].

The presence of two zeros in the BZ with the same phase winding is a topological *requirement* for the exciton order parameter, and is not an artifact of our effective LLL model. In an isolated band a with non-zero Chern number C_a, the phase of the electron creation operator $c^\dagger_{a,\mathbf{k}}$ cannot be chosen to be both continuous and single-valued over the BZ. In particular, it must wind $2\pi C_a$ times along the boundary of the BZ in a continuous gauge choice. This implies that the phase of $\Delta_{\mathbf{k}} = \langle c^\dagger_{+,\mathbf{k}} c_{-,\mathbf{k}}\rangle$ winds $2\pi(C_a - C_b) = 4\pi$ times along the BZ boundary for bands from opposite valleys with $C_a = 1$ and $C_b = -1$, which precisely corresponds to winding around two zeros with identical chirality.

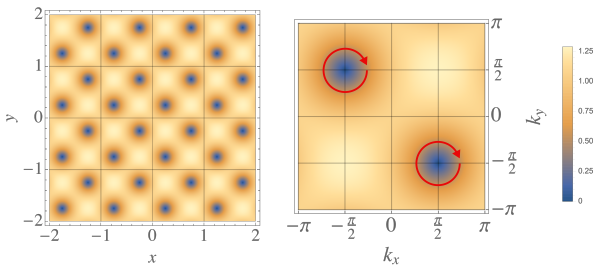

FIG. 2: The magnitude of the excitonic order parameter in real (left) and momentum (right) space (for $a = 1$, $\Delta_0 = 1$). The red circles denote identical phase-winding of $\Delta_{\mathbf{k}}$ at both nodal points.

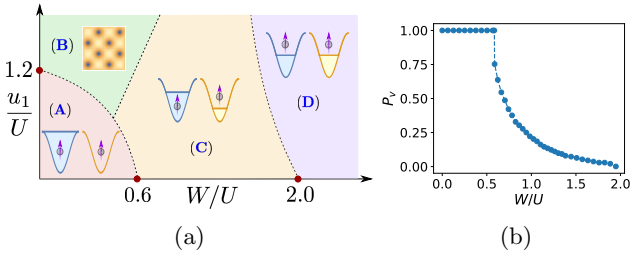

FIG. 3: (a) Approximate phase diagram of spin-polarized interacting electrons from opposite valleys in $C = \pm 1$ bands. The phases are (A) fully VP insulator, (B) exciton vortex lattice, (C) partially polarized metal or itinerant valley-ferromagnet, and (D) unpolarized metal. Everywhere within phases A and C, $R_{xy} \neq 0$. (b) Metal-insulator competition and the valley polarization P_v for isotropic interaction.

We now demonstrate that variational states with an exciton vortex lattice have higher energy than the VP state or the metal for small anisotropy u_1 in the interaction H^i. We consider the Slater determinant ground state $|\psi_{MF}\rangle$ of the mean-field Hamiltonian $H_{MF} = \sum_{\mathbf{k},\tau,\tau'} c^\dagger_{\mathbf{k},\tau} h_{\tau,\tau'}(\mathbf{k}) c_{\mathbf{k},\tau'}$, where $h_{\tau,\tau'}(\mathbf{k}) = \epsilon_{\mathbf{k}}\mathbb{1} + h\tau^z + \mathrm{Re}(\Delta_{\mathbf{k}})\tau^x + \mathrm{Im}(\Delta_{\mathbf{k}})\tau^y$. $|\psi_{MF}\rangle$ is characterized by the valley polarization P_v (determined by h) and an exciton vortex lattice of strength Δ_0, to be treated as variational parameters. The correlation matrix evaluated in this state takes the form of the projector $\langle c^\dagger_{\tau,\mathbf{k}} c_{\tau'\mathbf{k}'}\rangle = P_{\tau,\tau'}(\mathbf{k})\delta_{\mathbf{k},\mathbf{k}'}$, which can be used to evaluate the regularized HF energy density $e^{HF}(P_v, \Delta_0)$ of the variational state for a given microscopic interaction at a fixed filling $\nu = 1$. We find that the global minimum of e^{HF} lies at $|P_v| = 1$ and $\Delta_0 = 0$ for the insulator in the limit of flat bands and isotropic interaction ($u_1 = 0$) [51]. We next show that the states of interest, with a fixed valley polarization P_v at filling $\nu = 1$, are stable to the formation of an vortex lattice in presence of small interaction anisotropy. To do this, we consider the difference in energy density $e^{HF}(P_v, \Delta_0) - e^{HF}(P_v, 0)$ perturbatively in $|\Delta_0|$ for arbitrary repulsive interaction parametrized by u_0 and u_1; a positive difference would indicate that $\Delta_0 = 0$ corresponds to an energy minimum. For the polarized phase, we find

$$e^{HF}(1,\Delta_0) - e^{HF}(1,0) = \frac{1}{8h^2}\Big[\int_{\mathbf{k},\mathbf{q}} u_0(\mathbf{q})|\Delta_+ - \Delta_-|^2 + \int_{\mathbf{k},\mathbf{q}} u_1(\mathbf{q})|\Delta_+ + \Delta_-|^2 - 4u_1(\mathbf{0})\int_{\mathbf{k}} |\Delta_{\mathbf{k}}|^2\Big], \quad (5)$$

where $\Delta_\pm \equiv \Delta_{\mathbf{k}\pm\mathbf{q}/2}$ [51]. For a uniform exciton condensate, $\Delta_{\mathbf{k}} = \Delta_0$ and this energy difference is negative [51]. However, for an exciton order parameter formed with electrons and holes from opposite Chern bands, $\nabla_{\mathbf{k}}\Delta_{\mathbf{k}} \neq 0$. Therefore, when u_1 is sufficiently small compared to u_0 the energy of the state with non-zero $\Delta_{\mathbf{k}}$ is higher. So the VP state with $\Delta_0 = 0$, previously shown to be the ground state with an isotropic interaction for small W/u_0, is indeed robust to small interaction anisotropy. Analogous computations [51] show that the unpolarized metal ($P_v = 0 = \Delta_0$) is stable to the vortex lattice as well. An approximate phase diagram of our model for a short-range (LLL-projected) interaction anisotropy $u_1(\mathbf{q}) = u_1 e^{-\mathbf{q}^2 l_B^2/2}$ is presented in Fig. 3. For TBG, we expect $W/U \lesssim 0.2$ from the ratio of the bandwidth to the Coulomb interaction, and the anisotropy $u_1/U \lesssim 0.01$ to be small [51, 66], indicating a VP phase consistent with experiments [29, 67]. In the supplement, we numerically solve the mean-field equations for TBG on hBN at $\nu = 3$ and confirm that the spin and VP QAH state is indeed the ground state.

Valley Zeeman effect– Having argued in favor of a VP state at $\nu = 3$, we turn to the observed hysteresis in the $\nu = 3$ Hall conductance as a function of out-of-plane magnetic field B^z [29]. To this end, we compute the orbital g_v-factor for the TBG conduction bands. In a band τ without time-reversal electrons can carry a momentum-dependent orbital moment $m_{\tau,\mathbf{k}}$ [68, 69]. Time-reversal ensures that $m_{\tau,\mathbf{k}} = -m_{-\tau,-\mathbf{k}}$, which averaged over the mBZ produces a valley-Zeeman splitting $E = -g_v \frac{\tau^z}{2}\mu_B B^z$. We find that for $\Delta_b = 0, \Delta_t \sim 10 - 30$ meV, g_v ranges from approximately -2 to -6 [51]. Note that for $B^z > 0$, the $C = 1$ band comes down in energy. The sign of this effect is in agreement with the Landau fans of Refs. [29, 67].

Conclusion– We showed that broken inversion symmetry in TBG due to substrate (h-BN) coupling leads to two Chern bands per valley. Spontaneous polarization of holes in spin and valley space then leads to an AH state at $\nu = 3$. Using a LLL model, a HF analysis establishes a stable VP state as the ground state when the bandwidth is small compared to the interaction strength. The opposite Chern numbers for the two valleys precludes uniform inter-valley coherence. The resultant exciton vortex lattice structure reduces correlation energy gain and stabilizes valley-polarization. This result agrees with numerical work on a Hubbard model [70].

Note added– Recently, a quantized AHE with net Chern number $C = 1$ has been observed for a gapped insulator at $\nu = 3$ in TBG aligned with h-BN [67], consistent with our theoretical results. Quantized AHE arising from valley-Chern bands have also been observed [71] and proposed [72, 73] in other Moiré heterostructures, in

accordance with our phenomenological picture of interaction in nearly flat bands with opposite Chern numbers.

Acknowledgements– We thank Aaron Sharpe, Eli Fox and David Goldhaber-Gordon for discussions about their data and sharing their insights. We also thank Ryan Mishmash for explaining the details of Ref. 62 to two of us (SC and NB), and Ehud Altman, Senthil Todadri and Andrea Young for inspiring discussions. Our work overlaps with concurrent work by Y. Zhang, D. Mao and T. Senthil [74]. MZ and NB were supported by the DOE, office of Basic Energy Sciences under contract no. DE-AC02-05-CH11231. SC acknowledges support from the ERC synergy grant UQUAM via E. Altman.

[1] A. K. Geim and I. V. Grigorieva, "Van der waals heterostructures," Nature **499**, 419 EP – (2013).

[2] Rafi Bistritzer and Allan H. MacDonald, "Moiré bands in twisted double-layer graphene," Proceedings of the National Academy of Sciences **108**, 12233–12237 (2011).

[3] E. J. Mele, "Commensuration and interlayer coherence in twisted bilayer graphene," Phys. Rev. B **81**, 161405 (2010).

[4] J. M. B. Lopes dos Santos, N. M. R. Peres, and A. H. Castro Neto, "Continuum model of the twisted graphene bilayer," Phys. Rev. B **86**, 155449 (2012).

[5] J. M. B. Lopes dos Santos, N. M. R. Peres, and A. H. Castro Neto, "Graphene bilayer with a twist: Electronic structure," Phys. Rev. Lett. **99**, 256802 (2007).

[6] G. Trambly de Laissardière, D. Mayou, and L. Magaud, "Localization of dirac electrons in rotated graphene bilayers," *Nano Letters*, Nano Letters **10**, 804–808 (2010).

[7] S. Shallcross, S. Sharma, E. Kandelaki, and O. A. Pankratov, "Electronic structure of turbostratic graphene," Phys. Rev. B **81**, 165105 (2010).

[8] E. Suárez Morell, J. D. Correa, P. Vargas, M. Pacheco, and Z. Barticevic, "Flat bands in slightly twisted bilayer graphene: Tight-binding calculations," Phys. Rev. B **82**, 121407 (2010).

[9] Pilkyung Moon and Mikito Koshino, "Energy spectrum and quantum hall effect in twisted bilayer graphene," Phys. Rev. B **85**, 195458 (2012).

[10] Guohong Li, A. Luican, J. M. B. Lopes dos Santos, A. H. Castro Neto, A. Reina, J. Kong, and E. Y. Andrei, "Observation of van hove singularities in twisted graphene layers," Nature Physics **6**, 109 EP – (2009).

[11] A. Luican, Guohong Li, A. Reina, J. Kong, R. R. Nair, K. S. Novoselov, A. K. Geim, and E. Y. Andrei, "Single-layer behavior and its breakdown in twisted graphene layers," Phys. Rev. Lett. **106**, 126802 (2011).

[12] Wei Yan, Mengxi Liu, Rui-Fen Dou, Lan Meng, Lei Feng, Zhao-Dong Chu, Yanfeng Zhang, Zhongfan Liu, Jia-Cai Nie, and Lin He, "Angle-dependent van hove singularities in a slightly twisted graphene bilayer," Phys. Rev. Lett. **109**, 126801 (2012).

[13] I. Brihuega, P. Mallet, H. González-Herrero, G. Trambly de Laissardière, M. M. Ugeda, L. Magaud, J. M. Gómez-Rodríguez, F. Ynduráin, and J.-Y. Veuillen, "Unraveling the intrinsic and robust nature of van hove singularities in twisted bilayer graphene by scanning tunneling microscopy and theoretical analysis," Phys. Rev. Lett. **109**, 196802 (2012).

[14] Taisuke Ohta, Jeremy T. Robinson, Peter J. Feibelman, Aaron Bostwick, Eli Rotenberg, and Thomas E. Beechem, "Evidence for interlayer coupling and moiré periodic potentials in twisted bilayer graphene," Phys. Rev. Lett. **109**, 186807 (2012).

[15] Robin W. Havener, Yufeng Liang, Lola Brown, Li Yang, and Jiwoong Park, "Van hove singularities and excitonic effects in the optical conductivity of twisted bilayer graphene," Nano Letters **14**, 3353–3357 (2014), pMID: 24798502, https://doi.org/10.1021/nl500823k.

[16] R. de Gail, M. O. Goerbig, F. Guinea, G. Montambaux, and A. H. Castro Neto, "Topologically protected zero modes in twisted bilayer graphene," Phys. Rev. B **84**, 045436 (2011).

[17] Kazuyuki Uchida, Shinnosuke Furuya, Jun-Ichi Iwata, and Atsushi Oshiyama, "Atomic corrugation and electron localization due to moiré patterns in twisted bilayer graphenes," Phys. Rev. B **90**, 155451 (2014).

[18] A. O. Sboychakov, A. L. Rakhmanov, A. V. Rozhkov, and Franco Nori, "Electronic spectrum of twisted bilayer graphene," Phys. Rev. B **92**, 075402 (2015).

[19] Jeil Jung, Arnaud Raoux, Zhenhua Qiao, and A. H. MacDonald, "Ab initio theory of moiré superlattice bands in layered two-dimensional materials," Phys. Rev. B **89**, 205414 (2014).

[20] Dillon Wong, Yang Wang, Jeil Jung, Sergio Pezzini, Ashley M. DaSilva, Hsin-Zon Tsai, Han Sae Jung, Ramin Khajeh, Youngkyou Kim, Juwon Lee, Salman Kahn, Sajjad Tollabimazraehno, Haider Rasool, Kenji Watanabe, Takashi Taniguchi, Alex Zettl, Shaffique Adam, Allan H. MacDonald, and Michael F. Crommie, "Local spectroscopy of moiré-induced electronic structure in gate-tunable twisted bilayer graphene," Phys. Rev. B **92**, 155409 (2015).

[21] Shiang Fang and Efthimios Kaxiras, "Electronic structure theory of weakly interacting bilayers," Phys. Rev. B **93**, 235153 (2016).

[22] Y. Cao, J. Y. Luo, V. Fatemi, S. Fang, J. D. Sanchez-Yamagishi, K. Watanabe, T. Taniguchi, E. Kaxiras, and P. Jarillo-Herrero, "Superlattice-induced insulating states and valley-protected orbits in twisted bilayer graphene," Phys. Rev. Lett. **117**, 116804 (2016).

[23] Kyounghwan Kim, Ashley DaSilva, Shengqiang Huang, Babak Fallahazad, Stefano Larentis, Takashi Taniguchi, Kenji Watanabe, Brian J. LeRoy, Allan H. MacDonald, and Emanuel Tutuc, "Tunable moiré bands and strong correlations in small-twist-angle bilayer graphene," Proceedings of the National Academy of Sciences **114**, 3364–3369 (2017).

[24] Yuan Cao, Valla Fatemi, Ahmet Demir, Shiang Fang, Spencer L. Tomarken, Jason Y. Luo, Javier D. Sanchez-Yamagishi, Kenji Watanabe, Takashi Taniguchi, Efthimios Kaxiras, Ray C. Ashoori, and Pablo Jarillo-Herrero, "Correlated insulator behaviour at half-filling in magic-angle graphene superlattices," Nature **556**, 80 EP – (2018).

[25] Matthew Yankowitz, Shaowen Chen, Hryhoriy Pol-

shyn, K. Watanabe, T. Taniguchi, David Graf, Andrea F. Young, and Cory R. Dean, "Tuning superconductivity in twisted bilayer graphene," arXiv e-prints , arXiv:1808.07865 (2018), arXiv:1808.07865 [cond-mat.mes-hall].

[26] Alexander Kerelsky, Leo McGilly, Dante M. Kennes, Lede Xian, Matthew Yankowitz, Shaowen Chen, K. Watanabe, T. Taniguchi, James Hone, Cory Dean, Angel Rubio, and Abhay N. Pasupathy, "Magic Angle Spectroscopy," arXiv e-prints , arXiv:1812.08776 (2018), arXiv:1812.08776 [cond-mat.mes-hall].

[27] Youngjoon Choi, Jeannette Kemmer, Yang Peng, Alex Thomson, Harpreet Arora, Robert Polski, Yiran Zhang, Hechen Ren, Jason Alicea, Gil Refael, Felix von Oppen, Kenji Watanabe, Takashi Taniguchi, and Stevan Nadj-Perge, "Imaging Electronic Correlations in Twisted Bilayer Graphene near the Magic Angle," arXiv e-prints , arXiv:1901.02997 (2019), arXiv:1901.02997 [cond-mat.mes-hall].

[28] Guorui Chen, Lili Jiang, Shuang Wu, Bosai Lv, Hongyuan Li, Kenji Watanabe, Takashi Taniguchi, Zhiwen Shi, Yuanbo Zhang, and Feng Wang, "Gate-Tunable Mott Insulator in Trilayer Graphene-Boron Nitride Moiré Superlattice," arXiv e-prints , arXiv:1803.01985 (2018), arXiv:1803.01985 [cond-mat.mes-hall].

[29] Aaron L. Sharpe, Eli J. Fox, Arthur W. Barnard, Joe Finney, Kenji Watanabe, Takashi Taniguchi, M. A. Kastner, and David Goldhaber-Gordon, "Emergent ferromagnetism near three-quarters filling in twisted bilayer graphene," arXiv e-prints , arXiv:1901.03520 (2019), arXiv:1901.03520 [cond-mat.mes-hall].

[30] D. Efetov, "Cascade of superconducting domes and magnetic order around quarter filling in magic angle bilayer graphene," KITP program "Correlations in Moire Flat Bands" (2019).

[31] Jeil Jung, Ashley M. DaSilva, Allan H. MacDonald, and Shaffique Adam, "Origin of band gaps in graphene on hexagonal boron nitride," Nature Communications **6**, 6308 EP – (2015).

[32] B. Hunt, J. D. Sanchez-Yamagishi, A. F. Young, M. Yankowitz, B. J. LeRoy, K. Watanabe, T. Taniguchi, P. Moon, M. Koshino, P. Jarillo- Herrero, and R. C. Ashoori, "Massive Dirac Fermions and Hofstadter Butterfly in a van der Waals Heterostructure," Science **340**, 1427–1430 (2013), arXiv:1303.6942 [cond-mat.mes-hall].

[33] F. Amet, J. R. Williams, K. Watanabe, T. Taniguchi, and D. Goldhaber-Gordon, "Insulating Behavior at the Neutrality Point in Single-Layer Graphene," Phys. Rev. Lett. **110**, 216601 (2013), arXiv:1209.6364 [cond-mat.mes-hall].

[34] Menyoung Lee, John R. Wallbank, Patrick Gallagher, Kenji Watanabe, Takashi Taniguchi, Vladimir I. Fal'ko, and David Goldhaber-Gordon, "Ballistic miniband conduction in a graphene superlattice," Science **353**, 1526–1529 (2016), arXiv:1603.01260 [cond-mat.mes-hall].

[35] Matthew Yankowitz, Jeil Jung, Evan Laksono, Nicolas Leconte, Bheema L. Chittari, K. Watanabe, T. Taniguchi, Shaffique Adam, David Graf, and Cory R. Dean, "Dynamic band-structure tuning of graphene moiré superlattices with pressure," Nature (London) **557**, 404–408 (2018), arXiv:1707.09054 [cond-mat.mes-hall].

[36] A. A. Zibrov, E. M. Spanton, H. Zhou, C. Kometter, T. Taniguchi, K. Watanabe, and A. F. Young, "Even-denominator fractional quantum Hall states at an isospin transition in monolayer graphene," Nature Physics **14**, 930–935 (2018), arXiv:1712.01968 [cond-mat.str-el].

[37] Hakseong Kim, Nicolas Leconte, Bheema L. Chittari, Kenji Watanabe, Takashi Taniguchi, Allan H. MacDonald, Jeil Jung, and Suyong Jung, "Accurate Gap Determination in Monolayer and Bilayer Graphene/h-BN Moiré Superlattices," Nano Letters **18**, 7732–7741 (2018), arXiv:1808.06633 [cond-mat.mes-hall].

[38] Ya-Hui Zhang, Dan Mao, Yuan Cao, Pablo Jarillo-Herrero, and T. Senthil, "Nearly Flat Chern Bands in Moiré Superlattices," arXiv e-prints , arXiv:1805.08232 (2018), arXiv:1805.08232 [cond-mat.str-el].

[39] S. L. Sondhi, A. Karlhede, S. A. Kivelson, and E. H. Rezayi, "Skyrmions and the crossover from the integer to fractional quantum hall effect at small zeeman energies," Phys. Rev. B **47**, 16419–16426 (1993).

[40] J.P. Eisenstein, "Exciton condensation in bilayer quantum hall systems," Annual Review of Condensed Matter Physics **5**, 159–181 (2014).

[41] E. Tutuc, M. Shayegan, and D. A. Huse, "Counterflow Measurements in Strongly Correlated GaAs Hole Bilayers: Evidence for Electron-Hole Pairing," Phys. Rev. Lett. **93**, 036802 (2004), arXiv:cond-mat/0402186 [cond-mat.mes-hall].

[42] J. F. Dodaro, S. A. Kivelson, Y. Schattner, X. Q. Sun, and C. Wang, "Phases of a phenomenological model of twisted bilayer graphene," Phys. Rev. B **98**, 075154 (2018).

[43] Alex Thomson, Shubhayu Chatterjee, Subir Sachdev, and Mathias S. Scheurer, "Triangular antiferromagnetism on the honeycomb lattice of twisted bilayer graphene," Phys. Rev. B **98**, 075109 (2018).

[44] Jian Kang and Oskar Vafek, "Strong coupling phases of partially filled twisted bilayer graphene narrow bands," arXiv e-prints , arXiv:1810.08642 (2018), arXiv:1810.08642 [cond-mat.str-el].

[45] Masayuki Ochi, Mikito Koshino, and Kazuhiko Kuroki, "Possible correlated insulating states in magic-angle twisted bilayer graphene under strongly competing interactions," Phys. Rev. B **98**, 081102 (2018).

[46] Ming Xie and Allan H. MacDonald, "On the nature of the correlated insulator states in twisted bilayer graphene," arXiv e-prints , arXiv:1812.04213 (2018), arXiv:1812.04213 [cond-mat.str-el].

[47] Cenke Xu and Leon Balents, "Topological superconductivity in twisted multilayer graphene," Phys. Rev. Lett. **121**, 087001 (2018).

[48] Yu-Ping Lin and Rahul M. Nandkishore, "A chiral twist on the high-T_c phase diagram in Moir\'e heterostructures," arXiv e-prints , arXiv:1901.00500 (2019), arXiv:1901.00500 [cond-mat.str-el].

[49] Jianpeng Liu, Junwei Liu, and Xi Dai, "A complete picture for the band topology in twisted bilayer graphene," arXiv e-prints , arXiv:1810.03103 (2018), arXiv:1810.03103 [cond-mat.mes-hall].

[50] Ya-Hui Zhang and T. Senthil, "Bridging Hubbard Model Physics and Quantum Hall Physics in Trilayer Graphene/h-BN Moiré superlattice," arXiv e-prints , arXiv:1809.05110 (2018), arXiv:1809.05110 [cond-mat.str-el].

[51] See supplementary material, which contains Refs. [75–81].

[52] Takahiro Fukui, Yasuhiro Hatsugai, and Hiroshi Suzuki,

"Chern numbers in discretized brillouin zone: Efficient method of computing (spin) hall conductances," Journal of the Physical Society of Japan **74**, 1674–1677 (2005).

[53] Liujun Zou, Hoi Chun Po, Ashvin Vishwanath, and T. Senthil, "Band structure of twisted bilayer graphene: Emergent symmetries, commensurate approximants, and wannier obstructions," Phys. Rev. B **98**, 085435 (2018).

[54] Hoi Chun Po, Liujun Zou, Ashvin Vishwanath, and T. Senthil, "Origin of mott insulating behavior and superconductivity in twisted bilayer graphene," Phys. Rev. X **8**, 031089 (2018).

[55] Hoi Chun Po, Liujun Zou, T. Senthil, and Ashvin Vishwanath, "Faithful Tight-binding Models and Fragile Topology of Magic-angle Bilayer Graphene," arXiv e-prints , arXiv:1808.02482 (2018), arXiv:1808.02482 [cond-mat.str-el].

[56] Zhida Song, Zhijun Wang, Wujun Shi, Gang Li, Chen Fang, and B. Andrei Bernevig, "All "Magic Angles" Are "Stable" Topological," arXiv e-prints , arXiv:1807.10676 (2018), arXiv:1807.10676 [cond-mat.mes-hall].

[57] P. San-Jose, J. González, and F. Guinea, "Non-abelian gauge potentials in graphene bilayers," Phys. Rev. Lett. **108**, 216802 (2012).

[58] Grigory Tarnopolsky, Alex J. Kruchkov, and Ashvin Vishwanath, "Origin of Magic Angles in Twisted Bilayer Graphene," arXiv e-prints , arXiv:1808.05250 (2018), arXiv:1808.05250 [cond-mat.str-el].

[59] Nicola Marzari, Arash A. Mostofi, Jonathan R. Yates, Ivo Souza, and David Vanderbilt, "Maximally localized wannier functions: Theory and applications," Rev. Mod. Phys. **84**, 1419–1475 (2012).

[60] Xiao-Liang Qi, "Generic wave-function description of fractional quantum anomalous hall states and fractional topological insulators," Phys. Rev. Lett. **107**, 126803 (2011).

[61] Naokazu Shibata and Daijiro Yoshioka, "Stripe State in the Lowest Landau Level," Journal of the Physical Society of Japan **73**, 1 (2004), arXiv:cond-mat/0311213 [cond-mat.mes-hall].

[62] Ryan V. Mishmash, A. Yazdani, and Michael P. Zaletel, "Majorana lattices from the quantized Hall limit of a proximitized spin- orbit coupled electron gas," arXiv e-prints , arXiv:1811.05990 (2018), arXiv:1811.05990 [cond-mat.mes-hall].

[63] Z F Ezawa and G Tsitsishvili, "Quantum hall ferromagnets," Reports on Progress in Physics **72**, 086502 (2009).

[64] Titus Neupert, Luiz Santos, Shinsei Ryu, Claudio Chamon, and Christopher Mudry, "Topological hubbard model and its high-temperature quantum hall effect," Phys. Rev. Lett. **108**, 046806 (2012).

[65] Titus Neupert, Luiz Santos, Shinsei Ryu, Claudio Chamon, and Christopher Mudry, "Fractional topological liquids with time-reversal symmetry and their lattice realization," Phys. Rev. B **84**, 165107 (2011).

[66] Shubhayu Chatterjee, Nick Bultinck, and Michael P Zaletel, "Symmetry breaking and skyrmionic transport in twisted bilayer graphene," arXiv preprint arXiv:1908.00986 (2019).

[67] M. Serlin, C. L. Tschirhart, H. Polshyn, Y. Zhang, J. Zhu, K. Watanabe, T. Taniguchi, L. Balents, and A. F. Young, "Intrinsic quantized anomalous Hall effect in a moir\'e heterostructure," arXiv e-prints , arXiv:1907.00261 (2019), arXiv:1907.00261 [cond-mat.str-el].

[68] Di Xiao, Ming-Che Chang, and Qian Niu, "Berry phase effects on electronic properties," Rev. Mod. Phys. **82**, 1959–2007 (2010).

[69] Ming-Che Chang and Qian Niu, "Berry phase, hyperorbits, and the hofstadter spectrum: Semiclassical dynamics in magnetic bloch bands," Phys. Rev. B **53**, 7010–7023 (1996).

[70] Titus Neupert, Luiz Santos, Shinsei Ryu, Claudio Chamon, and Christopher Mudry, "Topological hubbard model and its high-temperature quantum hall effect," Phys. Rev. Lett. **108**, 046806 (2012).

[71] Guorui Chen, Aaron L. Sharpe, Eli J. Fox, Ya-Hui Zhang, Shaoxin Wang, Lili Jiang, Bosai Lyu, Hongyuan Li, Kenji Watanabe, and Takashi Taniguchi, "Tunable Correlated Chern Insulator and Ferromagnetism in Trilayer Graphene/Boron Nitride Moir\'e Superlattice," arXiv e-prints , arXiv:1905.06535 (2019), arXiv:1905.06535 [cond-mat.mes-hall].

[72] Xiaomeng Liu, Zeyu Hao, Eslam Khalaf, Jong Yeon Lee, Kenji Watanabe, Takashi Taniguchi, Ashvin Vishwanath, and Philip Kim, "Spin-polarized Correlated Insulator and Superconductor in Twisted Double Bilayer Graphene," arXiv e-prints , arXiv:1903.08130 (2019), arXiv:1903.08130 [cond-mat.mes-hall].

[73] Jong Yeon Lee, Eslam Khalaf, Shang Liu, Xiaomeng Liu, Zeyu Hao, Philip Kim, and Ashvin Vishwanath, "Theory of correlated insulating behaviour and spin-triplet superconductivity in twisted double bilayer graphene," arXiv e-prints , arXiv:1903.08685 (2019), arXiv:1903.08685 [cond-mat.str-el].

[74] Ya-Hui Zhang, Dan Mao, and T. Senthil, "Twisted Bilayer Graphene Aligned with Hexagonal Boron Nitride: Anomalous Hall Effect and a Lattice Model," arXiv e-prints , arXiv:1901.08209 (2019), arXiv:1901.08209 [cond-mat.str-el].

[75] D J Thouless, "Wannier functions for magnetic subbands," Journal of Physics C: Solid State Physics **17**, L325 (1984).

[76] R. Resta, "Theory of the electric polarization in crystals," Ferroelectrics **136**, 51–55 (1992).

[77] R. D. King-Smith and David Vanderbilt, "Theory of polarization of crystalline solids," Phys. Rev. B **47**, 1651–1654 (1993).

[78] Noah F. Q. Yuan and Liang Fu, "Model for the metal-insulator transition in graphene superlattices and beyond," Phys. Rev. B **98**, 045103 (2018).

[79] Jian Kang and Oskar Vafek, "Symmetry, maximally localized wannier states, and a low-energy model for twisted bilayer graphene narrow bands," Phys. Rev. X **8**, 031088 (2018).

[80] Mikito Koshino, Noah F. Q. Yuan, Takashi Koretsune, Masayuki Ochi, Kazuhiko Kuroki, and Liang Fu, "Maximally localized wannier orbitals and the extended hubbard model for twisted bilayer graphene," Phys. Rev. X **8**, 031087 (2018).

[81] Nick Bultinck, Eslam Khalaf, Shang Liu, Shubhayu Chatterjee, Ashvin Vishwanath, and Michael P. Zaletel, "Ground State and Hidden Symmetry of Magic Angle Graphene at Even Integer Filling," arXiv e-prints , arXiv:1911.02045 (2019), arXiv:1911.02045 [cond-mat.str-el].